IMPROVED PROPULSION MODELING FOR LOW-THRUST TRAJECTORY OPTIMIZATION

Jeremy M. Knittel[*]
Jacob A. Englander[†]
Martin T. Ozimek[‡]
Justin A. Atchison[§]
Julian J. Gould[¶]

Low-thrust trajectory design is tightly coupled with spacecraft systems design. In particular, the propulsion and power characteristics of a low-thrust spacecraft are major drivers in the design of the optimal trajectory. Accurate modeling of the power and propulsion behavior is essential for meaningful low-thrust trajectory optimization. In this work, we discuss new techniques to improve the accuracy of propulsion modeling in low-thrust trajectory optimization while maintaining the smooth derivatives that are necessary for a gradient-based optimizer. The resulting model is significantly more realistic than the industry standard and performs well inside an optimizer. A variety of deep-space trajectory examples are presented.

INTRODUCTION

Solar electric propulsion (SEP) is a means of propelling spacecraft that provides very high specific impulse (I_{sp}) at the expense of low thrust and high power requirements. The high I_{sp} of a SEP system enables many classes of mission that are difficult or impossible with chemical propulsion, including rendezvous with multiple asteroids, large-scale sample return, and delivery of very large payloads to the outer solar system. SEP trajectory design is more complex than chemical propulsion trajectory design and both the modeling and optimization techniques used in such designs are the subject of ongoing research.

SEP trajectory design is distinct from chemical propulsion trajectory design because the thrust levels are low and the maneuver durations are long. The impulse maneuver approximation does not hold and instead it is necessary to integrate the equations of motion across a maneuver arc as shown below.

$$\ddot{x} = \frac{-\mu}{r^3}x + \frac{T\left(P\left(r\right)\right)}{m}u_x \tag{1}$$

$$\ddot{y} = \frac{-\mu}{r^3}x + \frac{T\left(P\left(r\right)\right)}{m}u_y \tag{2}$$

$$\ddot{z} = \frac{-\mu}{r^3}x + \frac{T\left(P\left(r\right)\right)}{m}u_z \tag{3}$$

$$\dot{m} = \dot{m}\left(P\left(r\right)\right) \tag{4}$$

where T is maximum possible thrust force, $\dot{m}$ is available mass flow rate, P is power available to the thruster as a function of r, distance from the sun, and the u_i are components of a throttle control vector.

[*] Aerospace Engineer, Navigation and Mission Design Branch, NASA Goddard Space Flight Center, Member AAS
[†] Aerospace Engineer, Navigation and Mission Design Branch, NASA Goddard Space Flight Center, Member AAS
[‡] Aerospace Engineer, Applied Physics Laboratory, The Johns Hopkins University, Member AAS
[§] Aerospace Engineer, Applied Physics Laboratory, The Johns Hopkins University, Member AAS
[¶] Student, John Hopkins University

Electric propulsion systems are composed of a thruster, a power processing unit (PPU), and a propellant feed system. The propulsion system may be controlled by varying the input power, the beam voltage setting on the PPU, and/or a valve in the feed system that controls $\dot{m}$. PPUs and feed systems are typically designed with discrete choices of voltage and $\dot{m}$ in mind. The throttle table for an electric propulsion system therefore resembles a grid in voltage and $\dot{m}$. For example the NASA's evolutionary xenon thruster (NEXT) propulsion system [1] is designed to operate at a range of discrete voltages from 275 to 1800 V and a range of discrete mass flow rates from 1.85 mg/s to 5.76 mg/s. As currently designed, the NEXT system must be operated at points which appear on the voltage-$\dot{m}$ grid, each of which has been tested in laboratory conditions. Each set point provides a unique thrust, T, and specific impulse, I_{sp}. Other SEP systems are similar.

Thruster performance(T and $\dot{m}$) on power (P) is a major driver on the shape of the optimal trajectory for any SEP spacecraft whose distance from the sun, and therefore available power, change over the course of a mission. The more realistic the models for T and $\dot{m}$, the more closely the trajectory will resemble one that is actually physically acheivable. However there is a conflict between the need for realism in the model and the need for a model that is compatible with trajectory design software.

It is very challenging to model a propulsion system with discrete settings in the context of the gradient-based optimizers which are typically used to design low-thrust missions. Both direct and indirect optimization methods require a continuously differentiable force model, which conflicts with the discrete nature of the actual propulsion systems. Traditionally, low-thrust trajectory optimization software packages reduce the 2-dimensional throttle grid (each output is a function of both input power and voltage) to a 1-dimensional path (each output is a function of input power only). The models typically curve-fit the chosen subset, with a well-behaved "smooth" function such as an interpolating polynomial that is conducive to quasi-Newton, gradient-based NLP methods. Interpolating polynomials attempt to capture the aggregate behavior of the desired subset over the duration of the EP thrusting and moreover do not contain sharp changes in the first derivative. Such behavior prevents the thruster model from being the culprit of numerical over-sensitivity in the NLP search direction. In first-order methods, such numerical sensitivities can cause convergence "chatter" or outright limited robustness due to a lack of resolution in the quasi-Newton step. Smooth models are therefore the preferred choice for preliminary design searches, when the thruster firing history is unknown. A typical choice is a fifth-degree polynomial as a function of power available to the PPU:

$$\dot{m} = c_{m0} + c_{m1}P_a + c_{m2}P_a^2 + c_{m3}P_a^3 + c_{m4}P_a^4 + c_{m5}P_a^5 \tag{5}$$

$$\dot{T} = c_{t0} + c_{t1}P_a + c_{t2}P_a^2 + c_{t3}P_a^3 + c_{t4}P_a^4 + c_{t5}P_a^5 \tag{6}$$

where the c_t and c_m coefficients are used to approximate the thruster's stepped behavior over the range of power levels.

While inexpensive to evaluate and continuously differentiable, the industry-standard polynomial propulsion models are not very accurate. First, the true throttle grid is two-dimensional so one has to filter out throttle levels to select *a priori* which set of points to include in a 1-dimensional polynomial. In a particular mission, it may be beneficial to operate in a high-voltage, low-$\dot{m}$ regime for part of the trajectory and in a low-voltage, high-$\dot{m}$ regime for another part. Simplifying to a 1-dimensional set could therefore exclude the optimal trajectory. Second, the polynomials do not always accurately match the 1-dimensional sets of throttle points as shown in Figures 1 and 2. The particular polynomial models and throttle settings shown here are those that were provided for the NEXT propulsion system for the Discovery 14 contest [1]. The throttle settings used in these figures and throughout this work are provided by the NASA Glenn Research Center [2].

The actual throttle grid is discontinuous and therefore non-differentiable and incompatible with a gradient-based optimizer. The industry standard polynomial approximation is continuously differentiable but requires an *a priori* assumption about which path to follow through the throttle grid and, even once a path is chosen, is inaccurate relative to the actual capabilities of the propulsion system. It is therefore desirable to develop new models which:

1. more accurately model the EP system performance
2. are continuously differentiable

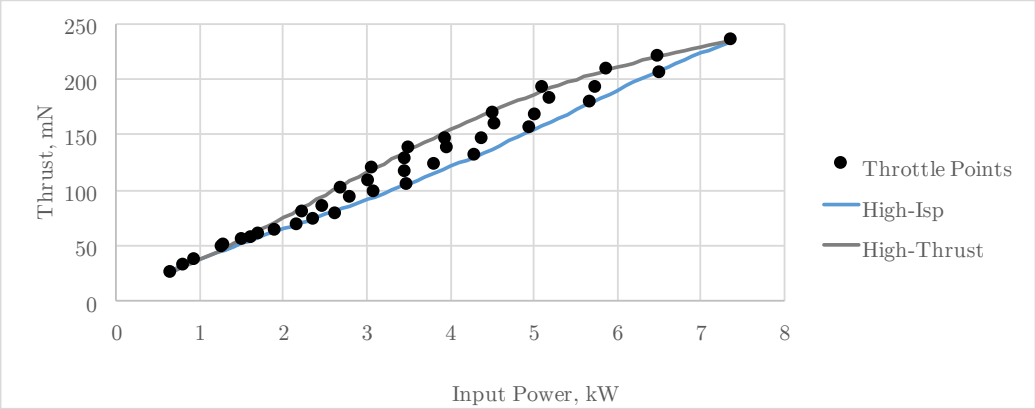

Figure 1: Polynomial thrust model compared to actual throttle grid

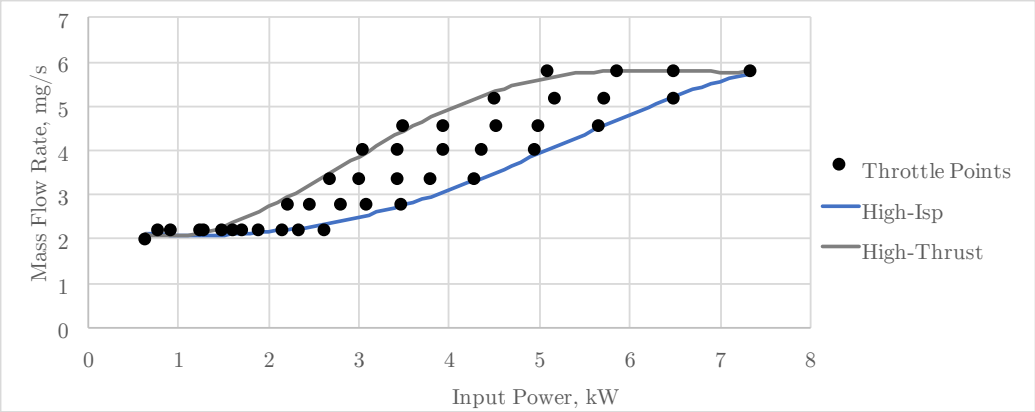

Figure 2: Polynomial thrust model compared to actual throttle grid

3. allow the optimizer to choose any point in the 2-dimensional throttle grid

In this work, novel propulsion models will be presented which satisfy some or all three of the above criteria. These new propulsion models are compatible with gradient-based optimizers but closely track the actual throttle grid. Multiple versions will be presented: some that require the analyst to choose a 1-dimensional path *a priori* and one that allows a gradient-based optimizer to choose points anywhere in the full 2-dimensional throttle grid. The new methods will be demonstrated on realistic mission designs and the results will be compared to those found by solving the same problem with the industry-standard polynomial propulsion model.

NON-DOMINATED SET

First, in order to choose 1-D paths through any arbitrary throttle box, we briefly introduce the concept of a non-dominated set. Similar to the formation of a pareto-front in multi-objective optimization, the distinct throttle settings of an electric thruster can be filtered to remove any throttle point which is worse than at least one other throttle point in both of the filtering objectives. Because all 1-D paths will become functions of input power, one of the filtering objectives is always input power. The second filtering objective is used to describe the 1-D path chosen. For example, to form the high-$\dot{m}$ non-dominated set, all throttle settings are removed which require both more input power and a higher mass flow rate of propellant than any other individual throttle setting. This can also be done to form the low-$\dot{m}$ set, the low-I_{sp} set and the high-thrust set (the high thrust set is typically similar or identical to the high-$\dot{m}$ set). These four non-dominated sets for

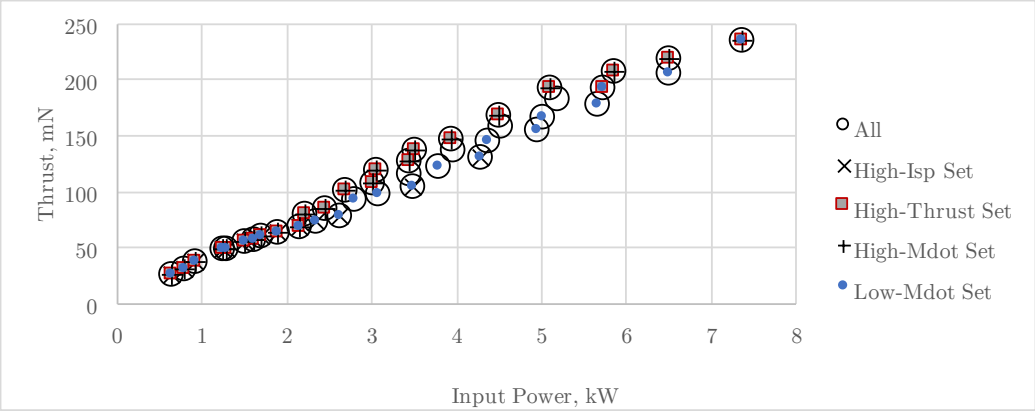

Figure 3: Non-dominated sets of the NEXT throttle settings

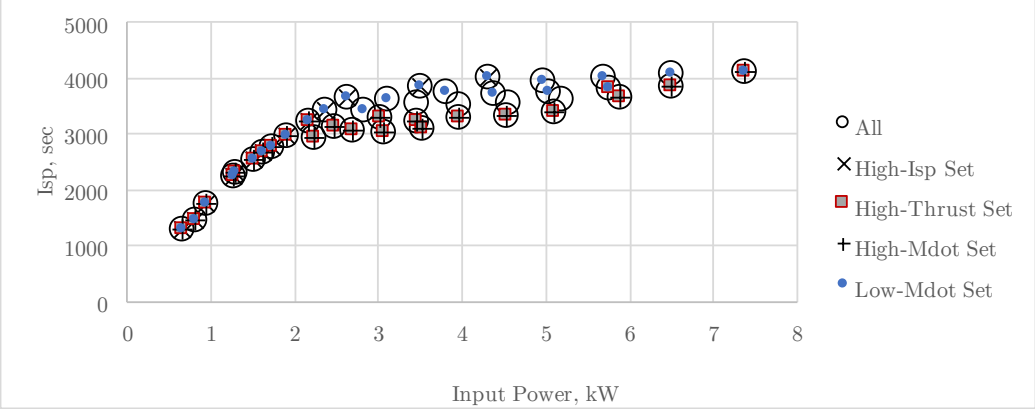

Figure 4: Non-dominated sets of the NEXT throttle settings

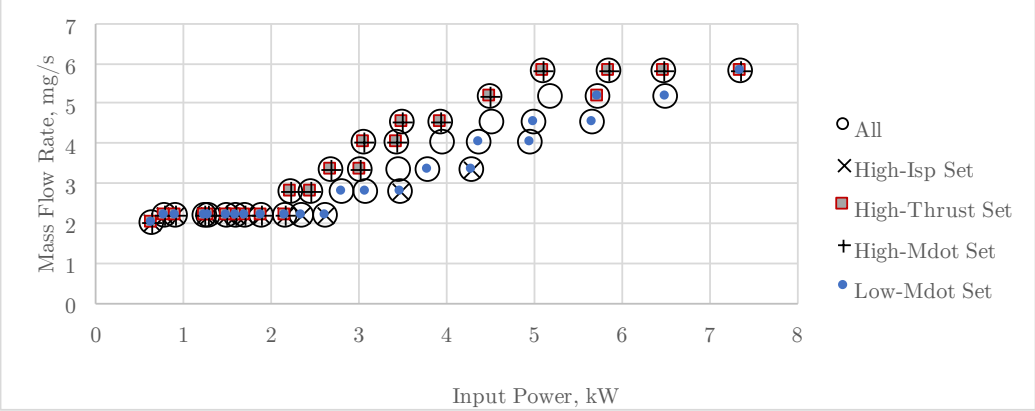

Figure 5: Non-dominated sets of the NEXT throttle settings

the NEXT propulsion system are shown in Figures 3, 4, and 5.

Note that these four sets represent the most logical choices for 1-D paths through a throttle grid, however, the 1-D models below could be used for any arbitrary set of throttle points that have unique levels of input power. The most useful 1-D paths will have monotonically increasing $\dot{m}$ and thrust (as input power increases) or else they will confuse the gradient-based optimizer and reduce its effectiveness.

POLYNOMIAL MODELS

Throttle Point Curve Fits

There are many ways to generate a polynomial fit to a throttle table. The most common approach is to perform a least-squares curve fit to a selected set of discrete throttle points. In this case, the predicted performance between throttle points is likely over or underestimated. Further, to accurately model the general shape of the throttle table, individual throttle points will likely be "missed" by the smooth curve.

The NEXT engine curve fit provided with the 2014 NASA Discovery Proposal is an example of a smooth model that approximated discrete set points (as shown in Figures 1 and 2). However, for trajectories that require many thruster set points, this choice results in an over-approximation of the thruster performance between steps (see Figure 6). A performance degradation when switching between smooth and more realistic stepped models can therefore be expected.

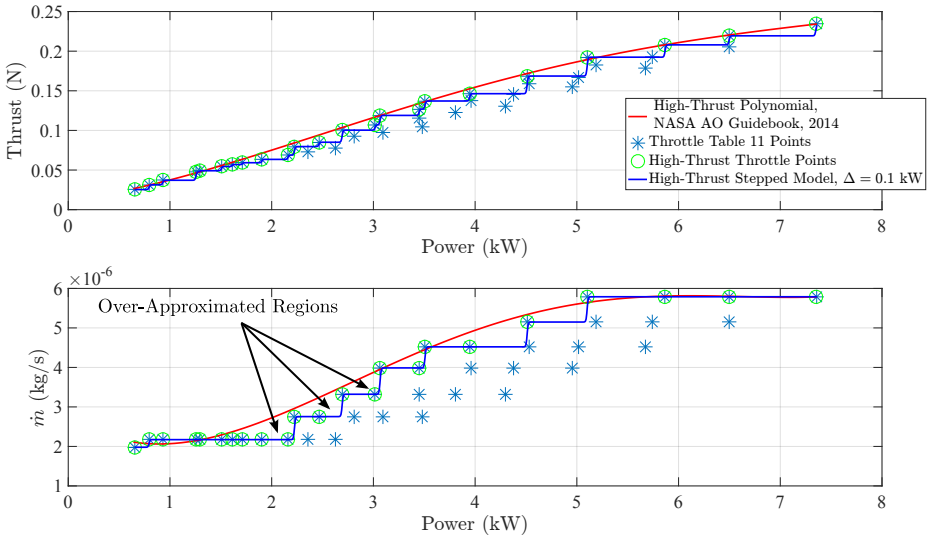

Figure 6: NEXT throttle table 11 and 1-D "high-thrust" approximations.

Further, the Discovery 14 polynomial models miss the throttle points in many locations. This is particularly true at low power levels, below 2 kW. This is significant because as a spacecraft moves farther out in the solar system, available power drops with $1/r^2$ and so, assuming a reasonable array size, any spacecraft going to the main asteroid belt or beyond will spend most of its time thrusting at low power levels. The low-power inaccuracy of the "standard" polynomial model will have negative consequences for outer-solar system mission design. Of course, one could construct polynomials that are more accurate in the low-power regime, but this would likely be at the expense of accuracy in other regions of the throttle grid, and in fact, any polynomial fit is likely to be inaccurate for certain ranges of input power. More importantly, any polynomial model also allows the propulsion system to operate at settings that do not appear in the throttle grid and are not physically realizable. This can result in trajectories that are overly optimistic about performance or worse, are also not physically realizable.

Integral Performance Matching

Here, we seek to derive a better approach for fitting the available thruster points. We evaluate the high-thrust and high-I_{sp} sets of NEXT throttle levels. Rather than derive a polynomial that matches the throttle points identically, we propose a method to approximate the overall behavior. In this approach, any single discrete point on the polynomial will have a nontrivial error, but the behavior overall (over many power levels) will more accurately model the throttle table.

A useful polynomial would have the following properties:

1. The integral or "area under the curve" over the range of available power is roughly preserved.
2. As possible, the integral over each throttle setting is preserved.
3. The initial and final throttle points are preserved.
4. The polynomial is monotonically increasing.

By preserving the integral of the throttle table, we ensure that the net performance neither over or underestimates the true performance. That is, the polynomial's overestimates must cancel its underestimates. Ideally, these errors will also be balanced over each throttle setting. Although any single throttle point may not be perfectly modeled, it's useful to capture the behavior at the minimum and maximum power settings. The minimum power setting is often encountered in deep space missions, and the maximum power setting is often the most efficient and encountered when power is sufficiently high. Any error in these two values could have a significant impact on overall accuracy. Finally, it's favorable that the polynomial be monotonically increasing because this better emulates the actual thruster behavior, in which increasing power always increases the available thrust and specific impulse. If the polynomial has a negative slope, an increase in power would result in poorer engine performance. This behavior could cause a trajectory optimizer to incorrectly favor a lower available power.

To this end, we construct a weighted least squares problem to incorporate these behaviors. A polynomial fit point is assigned to the middle of each vertical and horizontal step in the throttle table. These can be seen in Figure 7. These points are assigned a weight such that their sum is 1.0. An equation for the integral of the polynomial is used to constrain the sum of the errors. Two equations are added to constrain the initial and final points. Finally, the result is tuned by selectively constraining the slope of the polynomial at key points. This manual step prevents large overshoot behaviors. Table 1 gives the sets of least squares weights and relevant parameters. This table also includes a description of the constraint equations used.

The results of this process are given in Figures 7-10 and Tables 2 and 3. The performance of these polynomials is related to the polynomials presented in the NASA Discovery 2014 AO document. The custom polynomials derived here better balance the errors, where the NASA Discovery AO fits typically overestimate performance. The utility of these polynomials is further evaluated in two trajectory optimization examples given in sections below.

Table 1: Polynomial Weights and Inputs (based on EOL data)

	High Thrust		High Isp	
Parameter	Thrust	Mass Flow Rate	Thrust	Mass Flow Rate
Throttle Levels Incorporated	1-10,13,14,18,19,23,24,28,29,33,37-40		1-12,17,22,40	
Polynomial Order Selected	4	6	6	6
Number of Interior Fit Points	44	16	28	8
Interior Fit Point Weights	1.0/44	1.0/16	1.0/28	1.0/8
End Point Weights	25.0	25.0	25.0	25.0
Integral Equality Weight	0.01	0.01	0.01	0.01
Additional Slope Weight	None	10.0	10.0	10.0
Additional Slope Constraints		3.0E-07 kg/s/kW @ 0.653 kW	0.005 N/kW @ 5.829 kW	1.0E-09 kg/s/kW @ 0.653 kW
		1.0E-09 kg/s/kW @ 7.360 kW		1.0E-08 kg/s/kW @ 0.806 kW
				2.0E-07 kg/s/kW @ 2.132 kW
				2.0E-07 kg/s/kW @ 5.821 kW

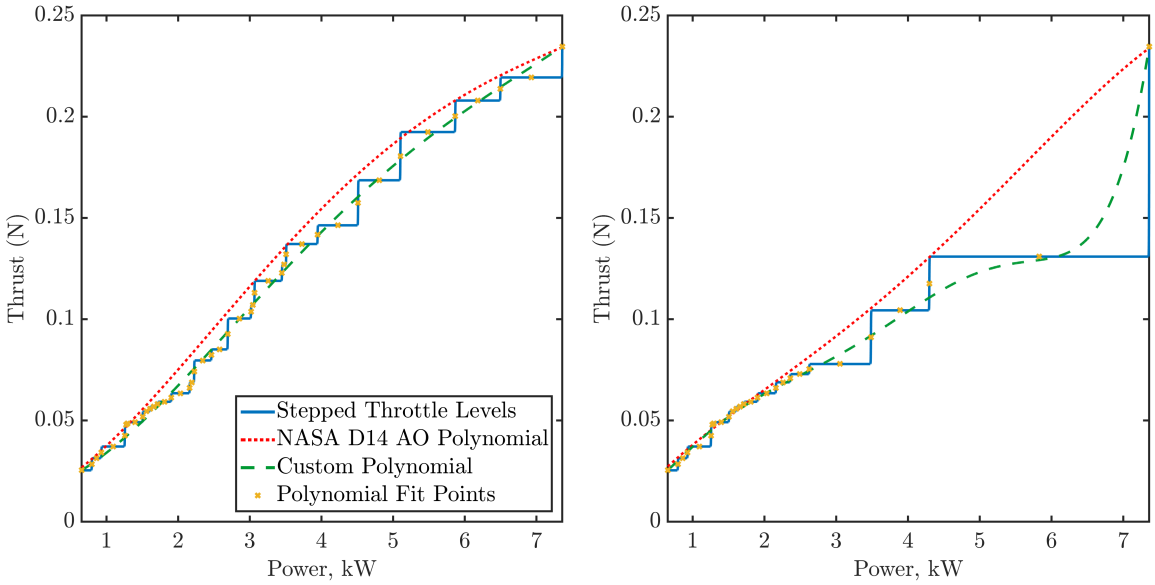

(a) High-Thrust Throttle Levels

(b) High-Isp Throttle Levels

Figure 7: Polynomial Fits to the NEXT Thrust Throttle Levels

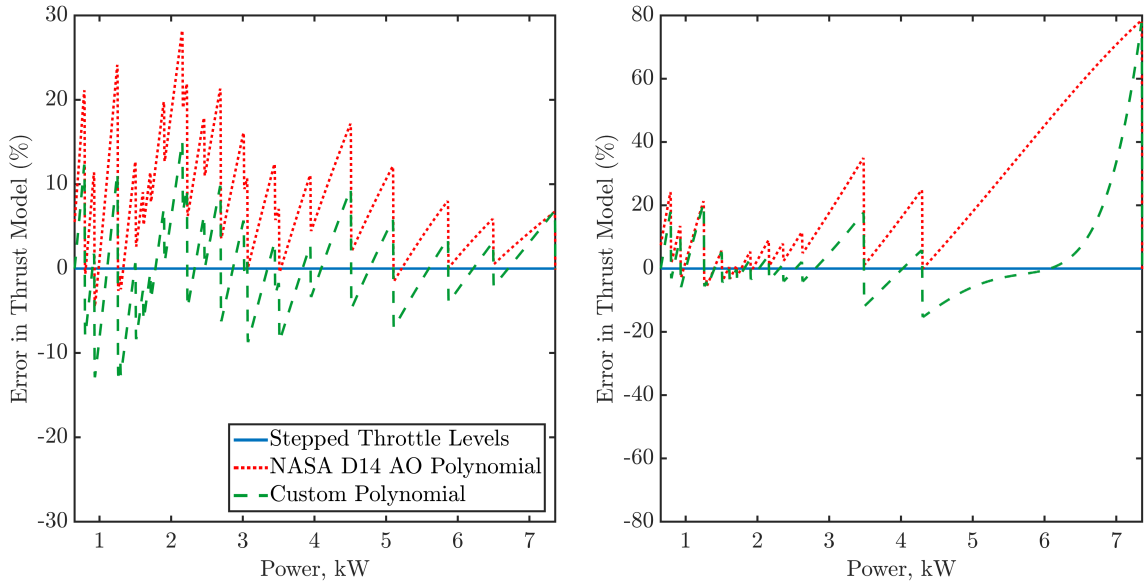

(a) High-Thrust Throttle Levels

(b) High-Isp Throttle Levels

Figure 8: Percent Error in Polynomial Fits to NEXT Thrust Levels

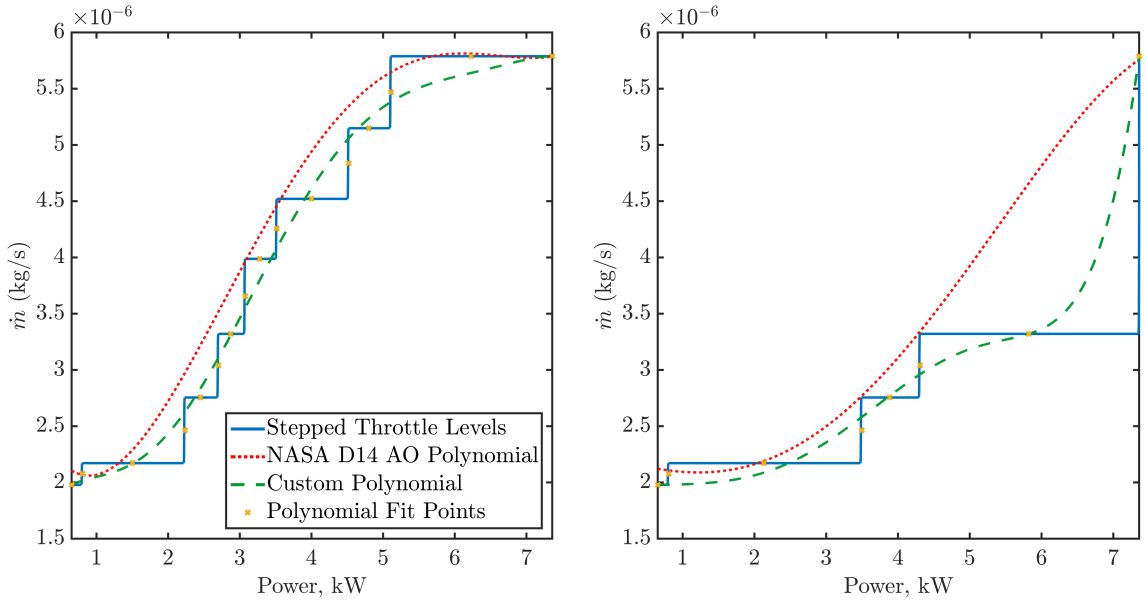

(a) High-Thrust Throttle Levels

(b) High-Isp Throttle Levels

Figure 9: Polynomial Fits to the NEXT Mass Flow Rate Throttle Levels

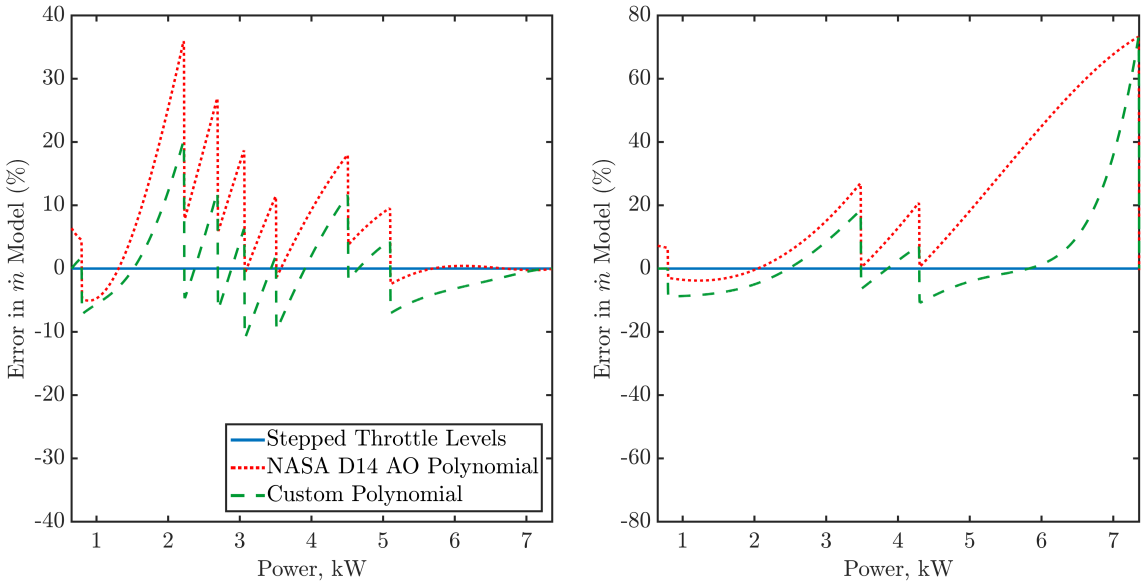

(a) High-Thrust Throttle Levels

(b) High-Isp Throttle Levels

Figure 10: Percent Error in Polynomial Fits to NEXT Mass-Flow Rate Levels

Table 2: Polynomial Fits to the NEXT Thrust Throttle Steps (based on EOL data)

	High Thrust		High Isp	
Parameter	NASA D14 AO	Custom	NASA D14 AO	Custom
c_{t0} (N)	1.19388817E-02	1.53147067E-02	3.68945763E-03	9.06756030E-03
c_{t1} (N/kW)	1.60989424E-02	7.77083385E-03	4.05432510E-02	7.96175232E-03
c_{t2} (N/kW^2)	1.14181412E-02	1.30817266E-02	-7.91621814E-03	4.22024750E-02
c_{t3} (N/kW^3)	-2.04053417E-03	-2.22362321E-03	1.72548416E-03	-3.02627265E-02
c_{t4} (N/kW^4)	1.19388817E-02	1.15864108E-04	-1.11563126E-04	9.28514190E-03
c_{t5} (N/kW^5)	0.0	0.0	0.0	-1.29785608E-03
c_{t6} (N/kW^6)	0.0	0.0	0.0	6.75040037E-05
Integral Error	+6.24%	+0.34%	+28.87%	4.25%
Initial Point Error	+5.51%	+0.00%	+7.39%	0.00%
Final Point Error	-0.13%	-0.00%	-0.32%	0.00%
Max Overestimate	28.2% (@2.14kW)	15.1% (@2.14kW)	78.4% (@7.35kW)	77.7% (@7.35kW)
Max Underestimate	4.5% (@0.94kW)	12.9% (@0.94kW)	5.4% (@1.30kW)	15.3% (@4.31kW)

Table 3: Polynomial Fits to the NEXT Mass-Flow Rate Throttle Steps (based on EOL data)

	High-Thrust		High-Isp	
Parameter	NASA D14 AO	Custom	NASA D14 AO	Custom
c_{m0} (kg/s)	2.75956482E-06	1.39733478E-06	2.22052155E-06	2.00382111E-06
c_{m1} (kg/s/kW)	-1.71102132E-06	1.83615417E-06	-1.80919262E-07	-1.06921486E-07
c_{m2} (kg/s/kW^2)	1.21670237E-06	-2.08514759E-06	2.77715756E-08	1.74340894E-07
c_{m3} (kg/s/kW^3)	-2.07253445E-07	1.13690887E-06	2.98873982E-08	-1.43304517E-07
c_{m4} (kg/s/kW^4)	1.10213671E-08	-2.61967933E-07	-2.91399146E-09	6.65953023E-08
c_{m5} (kg/s/kW^5)	0.0	2.72340756E-08	0.0	-1.22553728E-08
c_{m6} (kg/s/kW^6)	0.0	-1.06262899E-09	0.0	7.64533395E-10
Integral Error	+4.81%	-0.68%	+24.42%	4.43%
Initial Point Error	+6.39%	0.00%	+7.22%	0.00%
Final Point Error	-0.05%	0.00%	-0.52%	0.00%
Max Overestimate	43.3% (@2.20kW)	20.2% (@2.21kW)	73.2% (@7.35kW)	73.0% (@7.35kW)
Max Underestimate	2.4% (@5.04kW)	11.0% (@3.07kW)	3.8% (@1.22kW)	10.8% (@4.31kW)

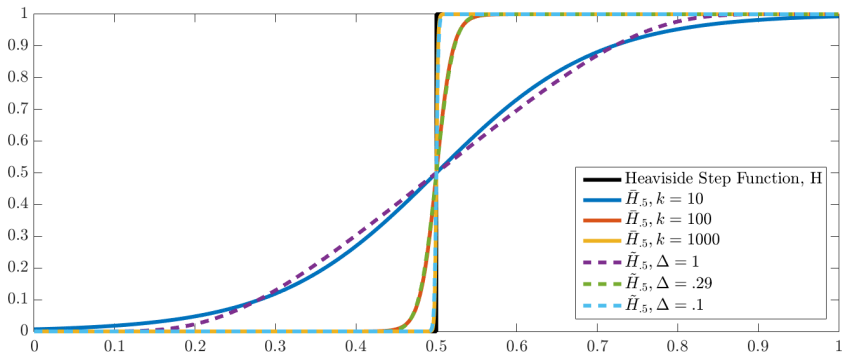

Figure 11: Heaviside step function and approximations

STEPPED MODELING

1-D Stepped Model

This section outlines a method to create a mathematical equation which has discontinuous increases from one throttle setting to another. This is possible using the so-called Heaviside step function (see equation 7). A Heaviside function has a value of one for an input greater than or equal to a critical value, and zero for all other inputs. Each throttle point can be modelled with a Heaviside function that turns its value of thrust and mass flow rate "on" at its input thruster power. However, the magnitude of each Heaviside function only reflects a step increase over the previous throttle point's value. Let P_a be the continuously defined power available to the PPU, and $x_i \in \{x_1, x_2, \ldots, x_n\}$ denote either a mass flow rate or thrust magnitude set point associated with a power level $P_i \in \{P_1, P_2, \ldots, P_n\}$.

$$H_i = \begin{cases} 1 & \text{if } S_i \geq 0 \\ 0 & \text{if } S_i < 0 \end{cases} \tag{7}$$

$$S_i = P_a - P_i \tag{8}$$

The mass flow rate or thrust magnitude available at a given power available is then:

$$x = x_1 H_1 + \sum_{i=2}^{n} (x_i - x_{i-1}) H_i \tag{9}$$

Implementing equation 9 solves the first of the three criteria set out above, in that the model output perfectly matches the capability of the thruster at any input power. However, this model does not meet the second criteria. The differentiability problem is solved by replacing the discontinuous Heaviside functions above with a logistics function (Figure 11) which smoothly and continuously approximates step increases:

$$\bar{H}_i = \frac{1}{1 + e^{-kS_i}} \tag{10}$$

The parameter k, or throttle sharpness, determines how closely the logistics function models the step increase of a Heaviside function.

The net model which solves the first two criteria set out above we name the 1-D stepped model and is presented in equation :

$$x = x_1 \bar{H}_1 + \sum_{i=2}^{n} (x_i - x_{i-1}) \bar{H}_i \tag{11}$$

and the relevant analytical derivative is:

$$\frac{dx}{dP_a} = kx_1\bar{H}_1^2 e^{-kS_i} + k\sum_{i=2}^{n}(x_i - x_{i-1})\bar{H}_i^2 e^{-kS_i} \tag{12}$$

For a conceptual example of how this model works, let throttle levels 1 and 2 are consecutive members of a chosen non-dominated set requiring 1 kW and 2 kW to operate and generating 100 mN and 150 mN of thrust, respectively. As the power available to the thrusters increases past 2 kW, the Heaviside function for throttle level 2 switches "on". However, because the engine is already outputing 100 mN from throttle point 1, the step increase associated with throttle level 2's Heaviside function is only 50 mN resulting in a net output of 150 mN. The input power has not yet been reached for any of the other throttle levels, so they do not contribute to the "net" thrust and mass flow rate, even though they are summed over.

For values of k greater than 1000, the Heaviside step function and the logistics function approximation are nearly indistinguishable. However, this has negative effects for the differentiability of the function. As k increases, the derivatives with respect to power in the "flat" regions grow closer and closer to zero, and the derivative for $P_a = P_i$ becomes larger and larger. In practice, the value of k should be chosen for the specific throttle box, and the capability of the gradient-based optimizer. Further, there could be a separate value of k chosen for each throttle level, if so desired, but here we assume that one identical value is used everywhere.

1-D Stepped Model with Smoothing Radius

One drawback to the 1-D method described above is that the parameter to control the steepness of the discontinuity approximation, k, is non-dimensional. It is often preferable to have this parameter in units of the independent variable, input power. This can be accomplished with a different Heaviside approximation. If we define a smoothing radius, Δ, then the Heaviside approximation becomes:

$$\tilde{H}_i = \frac{F_{i,1}}{F_{i,1} + F_{i,2}} \tag{13}$$

$$F_{i,1} = \begin{cases} e^{\left(\frac{-1}{S_i + \Delta/2}\right)} & S_i > -\Delta/2 \\ 0 & S_i \leq -\Delta/2 \end{cases} \tag{14}$$

$$F_{i,2} = \begin{cases} e^{\left(\frac{-1}{\Delta/2 - S_i}\right)} & S_i < \Delta/2 \\ 0 & S_i \geq \Delta/2 \end{cases} \tag{15}$$

For gradient-based algorithms, the derivative of equation with $\tilde{H}$ replacing $\bar{H}$ is readily available as:

$$\frac{dx}{dP_a} = x_1\frac{d\tilde{H}_1}{dP_1} + \sum_{i=2}^{n}(x_i - x_{i-1})\frac{d\tilde{H}_i}{dP_i} \tag{16}$$

$$\frac{\partial H_i}{\partial P} = \frac{(\frac{\partial F_{i,1}}{\partial P})F_{i,2} - (\frac{\partial F_{i,2}}{\partial P})F_{i,1}}{(F_{i,1} + F_{i,2})^2} \tag{17}$$

$$\frac{\partial F_{i,1}}{\partial P} = \begin{cases} \frac{1}{(S_i + \Delta/2)^2} e^{\left(\frac{-1}{S_i + \Delta/2}\right)} & S_i > -\Delta/2 \\ 0 & S_i \leq -\Delta/2 \end{cases} \tag{18}$$

$$\frac{\partial F_{i,2}}{\partial P} = \begin{cases} \frac{-1}{(\Delta/2 - S_i)^2} e^{\left(\frac{-1}{\Delta/2 - S_i}\right)} & S_i < \Delta/2 \\ 0 & S_i \geq \Delta/2 \end{cases} \tag{19}$$

In contrast to the sharpness, k, approach, this approximation allows direct control over the power smoothing radius Δ of the set points. Choice of an appropriate value is again a compromise between accuracy and numerical sensitivity. A value of $\Delta = 0.1$ kW in trial problems generally satisfies these competing objectives.

2-D Stepped Model

The 1-D model solves the first two of our objectives, but not the third, that of allowing the optimizer to choose any throttle level within the full grid. This will first necessitate the introduction of an additional control variable. Any parameter which has a discrete value at each throttle setting could be used (thrust, I_{sp}, voltage, current, $\dot{m}$), but the fewer settings that the control variable has, the more effective it will be. In this work, we will continue to use the NEXT thruster as an example, and as such, $\dot{m}$, voltage, or current are the most logical control variables. As any of these control variables could be used (with slightly varying effectiveness), we will simply use $u_{command}$ to represent whichever control variable was selected.

Similiar to the 1-D model, the 2-D model will use the logistics function approximation to the Heaviside step function to turn each throttle point "on", however in the 2-D model, each throttle point will use Heaviside functions to turn the throttle level "off" as well. Because of the increased dimensionality, there is no *a priori* order to the throttle points. From a given pair of P_a and $u_{command}$, depending which (or both) control variable changes to move in the throttle grid, many different throttle levels could be the next to be activated.

Again, the net thrust output by the EP system is a summation of the thrust and mass flow rate functions for all throttle points. Assuming that the command variable is voltage, the thrust and mass flow rate generated is:

$$x = \sum_{i=1}^{n} x_i (\bar{H}_{P_{on,i}} - \bar{H}_{P_{off,i}})(\bar{H}_{V_{on,i}} - \bar{H}_{V_{off,i}}) \tag{20}$$

Recalling that $\bar{H}_P$ was defined in equation 10, we simply now add a more detailed subscript to distinguish between the command variable and power available. $\bar{H}_V$ takes the same form, simply with critical values of voltage instead of power:

$$\bar{H}_{V_i} = \frac{1}{1 + e^{-k(u_{voltage} - V_i)}} \tag{21}$$

As the throttle table is initally parsed, the values of $P_{on,i}$, $P_{off,i}$, $\dot{m}_{on,i}$, and $\dot{m}_{off,i}$ are found for each throttle level. The "on" value for each throttle level always corresponds to the operating conditions of the given throttle level. Power and the command variable are sorted in slightly different manners to determine the "off" condition. To explain, continue assuming that voltage is used as the command variable. All of the throttle points are sorted by their required voltage input. For a given throttle level, the critical value of voltage which turns it "off" by way of a negative Heaviside step function is the next greater voltage level, regardless of required input power. On the other hand, the critical available power is found by sorting only those throttle levels with identical input voltage and selecting the next greater input power. Given both sorting methods, the 2-D model will be most effective by selecting a command variable with the fewest discrete levels. For example, even though the NEXT thruster has 40 total throttle settings, there are only 12 potential values of voltage and 8 potential values of mass flow rate.

Finally, the derivatives with respect to decision variables are defined in the following equations (again with voltage as the command variable):

$$\frac{\partial x}{\partial P_a} = k \sum_{i=1}^{n} x_i (\bar{H}_{V_{on,i}} - \bar{H}_{V_{off,i}})(e^{-k(P_a - P_{on,i})} \bar{H}^2_{P_{on,i}} - e^{-k(P_a - P_{off,i})} \bar{H}^2_{P_{off,i}}) \tag{22}$$

$$\frac{\partial x}{\partial u_{voltage}} = k \sum_{i=1}^{n} x_i (\bar{H}_{P_{on,i}} - \bar{H}_{_{off,i}})(e^{-k(u_{voltage} - V_{on,i})} \bar{H}^2_{V_{on,i}} - e^{-k(u_{voltage} - V_{off,i})} \bar{H}^2_{V_{off,i}}) \tag{23}$$

CASE STUDIES

Ceres

As a first example, consider a hypothetical 2024 Earth-Mars-Ceres rendezvous with the assumptions of Table 4. The results of the trajectory optimizations are qualitatively very similar, however the over-approximation of the standard polynomial model creates a major mismatch in trajectory performance against all alternative propulsion models (see Figure 12 and Table 5).

Table 4: Assumptions for Earth-Mars-Ceres Rendezvous Mission

Option	Value
Optimization Objective	max. final mass
Launch date boundaries	1/31/2024 – 10/30/2024
Flyby date boundaries	7/30/2025 – 9/28/2025
Flight time upper bound	7 years (2555 days)
Propellant upper bound	500 kg
Arrival condition at Mars	flyby
Arrival condition at Ceres	rendezvous
Launch vehicle	Atlas V 401
Launch asymptote declination bounds	$[-28.5°, 28.5°]$ (Kennedy Space Center)
Post-launch coast duration	30 days
Pre-flyby coast duration	30 days
Solar array P_0	15 kW
Solar array coefficients γ_i	$[1.0, 0, 0, 0, 0]$
Spacecraft power coefficients $a_{s/c} - c_{s/c}$	$[1.0, 0, 0]$
Propulsion system	varies by trial
Duty cycle	90%
Thrust scale factor	100%
Power margin	0%
Number of time steps per phase	100

All trials nearly reach the propellant throughput limit, but the stepped-models (Trials #2 and #3) are less capable, leading to a lower launch mass to push the spacecraft through a similar trajectory. The over estimation is clear from Figure 14, as the stepped models show that it is impossible to fully utilize all of the available power. The mismatch becomes most significant during the period following the Mars flyby, where significant periods of thrusting at lower throttle settings occur. The gradual shifting between throttle points exacerbates the modeling disagreement between the smooth and stepped models.

The 2-D stepped model (Trial #3) provides only roughly a 1 kg improvement over the 1-D stepped model in both delivered mass and propellant usage. The throttle settings are somewhat different however, as the optimization algorithm chooses some throttle settings from the high-Isp set which are not available for the 1-D optimization (see Figure 13). The differences can also be seen with careful observation of Figure 14, as the 2-D solution thrusts for slightly longer on both phases of the journey and utilizes increased power, but due to the higher Isp of the throttle levels used, less propellant is consumed. In this instance, the 2-D solution was found by using the 1-D stepped solution as an initial guess, and the initial guess was actually feasible for the 2-D optimization run, as the command variable values were explicitly calculated to match the 1-D solution. It is therefore not surprising that the 2-D solution matches so closely to the 1-D solution and in fact, only one additional throttle setting was used, as seen in Figure 13. In order to retain the utility of the initial guess, the throttle sharpness was kept at k = 10000. As mentioned this causes the derivatives to be very small in most regions of the design space and very large as the throttle points switch. The net effect is that the gradient based NLP solver has numerical difficulty making significant improvement away from the initial guess. Further improvement could likely be found with an improved global search capability, however, this does not change the slight shortcoming of the 2-D model. As the throttle sharpness parameter, k, decreases or the smoothing radius, Δ, increases, the 1-D stepped model decreases in accuracy at a much slower rate than does the 2-D model. Because the 1-D model only uses step increases from the previous throttle point, it is much less sensitive to k. This situation could likely be avoided by developing initial guesses with a lower value of k, however this would require increased computation time.

The fourth trial, utilizing the equal area integral approximation of the high-thrust throttle points in the stepped model, significantly improves the trajectory agreement with the 1-D stepped model, including the critical event dates, launch C3, and most importantly, the optimal final mass which disagrees with the 1-D stepped model by only 3.95 kg.

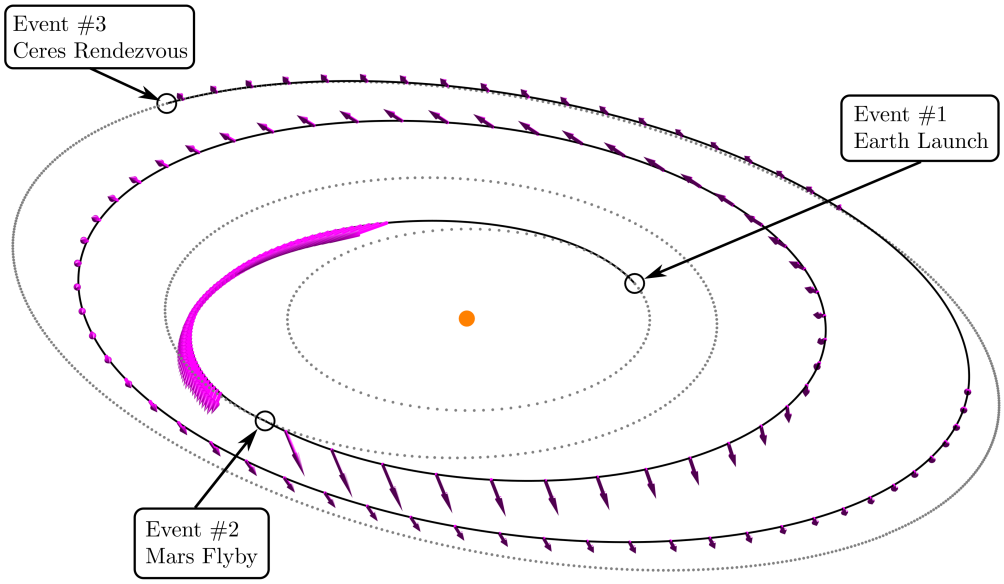

Figure 12: Earth-Mars-Ceres trajectory example. Due to qualitative similarities, only trial #1 is shown.

	Trial 1	Trial 2	Trial 3	Trial 4
Engine Model	2014 Discovery AO high-thrust polynomial	1-D stepped high-thrust, $\Delta = 0.1$ kW	2-D stepped, k = 10000	equal area integral polynomial
Launch Date	9/26/2024	9/24/2024	9/25/2024	9/25/2024
Launch C3	10.55 km^2/s^2	11.09 km^2/s^2	11.26 km^2/s^2	10.74 km^2/s^2
Launch DLA	6.1°	-1.4°	$-.85^\circ$	1.6°
Launch Mass	2057.84 kg	1976.04 kg	1976.70 kg	1979.99 kg
Mars Flyby Date	7/30/2025	7/30/2025	7/30/2025	7/30/2025
Mars Flyby v_∞	2.46 km/s	2.70 km/s	2.70 km/s	2.66 km/s
Mass at Flyby	1993.05 kg	1895.34 kg	1896.47 kg	1895.66 kg
Mars Flyby Altitude	300 km	300 km	300 km	300 km
Ceres Arrival Date	9/25/2031	9/23/2031	9/24/2031	9/24/2031
Total Flight Time	2555 days	2555 days	2555 days	2555 days
Mass After Rendezvous	1557.84 kg	1476.04 kg	1477.38 kg	1479.99 kg
Total Propellant Use	500.00 kg	500.00 kg	499.32 kg	500.00 kg

Table 5: Trajectory data for the Earth-Mars-Ceres example

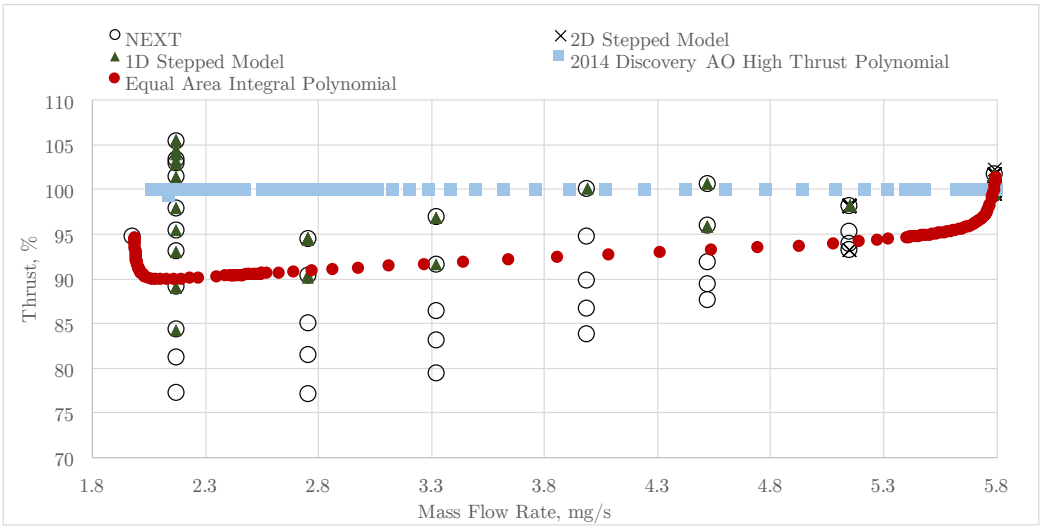

Figure 13: Comparison of engine model outputs for the sample Ceres mission. Nondimensional thrust is plotted, scaled by the value of the AO polynomial at any given mass flow rate.

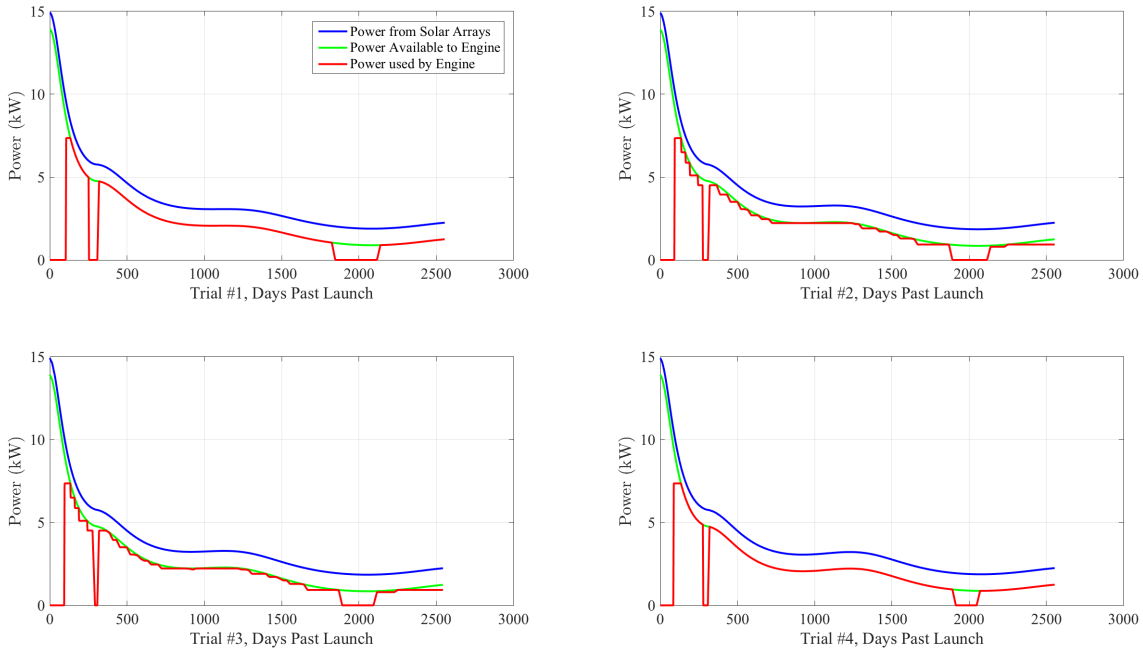

Figure 14: Comparison of power usage for the four trials

Trojan Tour

A notional SEP mission to the Trojan asteroids Nauplius and Odysseus is used as the second benchmark case for the new propulsion models. This benchmark is particularly timely because the "Trojan Tour and Rendezvous" is listed as one of the acceptable targets in the New Frontiers 4 Announcement of Opportunity that was recently released by NASA [3]. As a mission of current interest, the Trojan Tour and Rendezvous is an ideal case with which to validate a new design tool that may be used to propose such missions. The Announcement of Opportunity states that the Trojan Tour and Rendezvous "is intended to examine two or more small bodies sharing the orbit of Jupiter, including one or more flybys followed by an extended rendezvous with a Trojan object." Accordingly, our benchmark mission performs a flyby of the magnitude 10.7 Trojan 9712 Nauplius before rendezvousing with 1143 Odysseus, which at magnitude 7.93 is one of the largest Trojans. This benchmark is appropriate for comparing the NEXT "stepped" propulsion models to the industry-standard polynomials because it exercises the propulsion model at a wide range of available power.

The assumptions for the benchmark mission to Nauplius and Odysseus are listed in Table 6. The second benchmark mission was designed using the Evolutionary Mission Trajectory Generator (EMTG) [4, 5]. EMTG uses a form of global search known as monotonic basin hopping to generate initial guesses, but each individual optimization run requires a gradient based NLP solver. For this reason, it is crucial that changes in the engine model performance be smooth with continuous derivatives. The mission was designed using both polynomial models and both the 1-D and 2-D stepped models.

Table 7 lists the major events in all four versions of the mission, and Figure 15 is a plot of the optimal trajectory. Note that all four optimal trajectories look qualitatively similar in a Universe view, so only Trial #2 (1-D stepped model) is shown. Finally, Figure 16 displays the EP system outputs used in each of the trajectories.

As expected, the solution found using the industry standard polynomial severely overestimates the dry mass that can be delivered to an Odysseus rendezvous by roughly 9%. On the other hand, in this case, the improved polynomial model, while much more accurate, still over estimates the 1-D NEXT system capability by 1.8%, but the 2-D capability by only .08%. The equal area integral polynomial is clearly a preferable polynomial model for early stage design.

The 2-D stepped model allows more mass to be delivered to the Trojan rendezvous than the 1-D stepped model, and the solutions are 1.7% separated. An improvement is to be expected, as the optimizer has an increased number of throttle settings to choose from. However, it is difficult to predict the amount of improvement. Unlike the Ceres mission, the optimizer selected many throttle settings that were not on the 1-D non-dominated path. This is primarily due to the spacecraft having two thrusters onboard. Given that the solar arrays were sized in order to allow maneuvering at 5 AU, near the Trojan asteroid cloud, there is excess power available to fire two thrusters when the spacecraft is still near Earth, and with two thrusters, the spacecraft is able to get sufficient thrust capability at the high Isp settings, rather than needing to use solely the high thrust settings.

One unexpected result from this comparison study is that trials 2,3 and 4 all found optimal solutions which underloaded the Atlas 551 launch vehicle by roughly 2000 kg. Further, despite launching with lower C_3, both stepped solutions require less propellant than the trial #1 solution. This is not necessarily surprising for the 2-D solution which has access to a greater number of throttle control settings, some of which are more fuel efficient, but this is unexpected for the 1-D solution. In many cases, switching from a polynomial solution to a stepped solution not only decreases the mass deliverable to the final orbit, but also increases the propellant required.

While the solution for all four trials activated the total flight time constraint, the date of Nauplius intercept varies by over one month and demonstrates the greatest variability in the four trajectory timelines. Given the variability, yet the qualitative similarity in the trajectories, the overall trajectory does not appear to be highly sensitive to the flyby date. A further constraint could likely force the timelines to match exactly, with a similar variation in mass history.

Table 6: Assumptions for the benchmark mission to Nauplius and Odysseus

Option	Value
Launch window open date	1/1/2024
Launch window close date	12/31/2024
Flight time upper bound	12 years
Arrival condition at Nauplius	flyby
Arrival condition at Odysseus	rendezvous
Launch vehicle	Atlas V 551
Launch asymptote declination bounds	$[-28.5, 28.5]$ (Kennedy Space Center)
Post-launch coast duration	60 days
Pre-flyby coast duration	30 days
Post-flyby coast duration	30 days
Solar array $P0$	40 kW
Solar array coefficients γ_i	$[1, 0, 0, 0, 0]$
Spacecraft power coefficients $a_{s/c} - c_{s/c}$	$[0.8, 0, 0]$
Propulsion system	2 NEXT engines
Throttle Logic	minimum number of thrusters
Duty cycle	90%
Thrust scale factor	99%
Power margin	15%
Number of time steps per phase	20

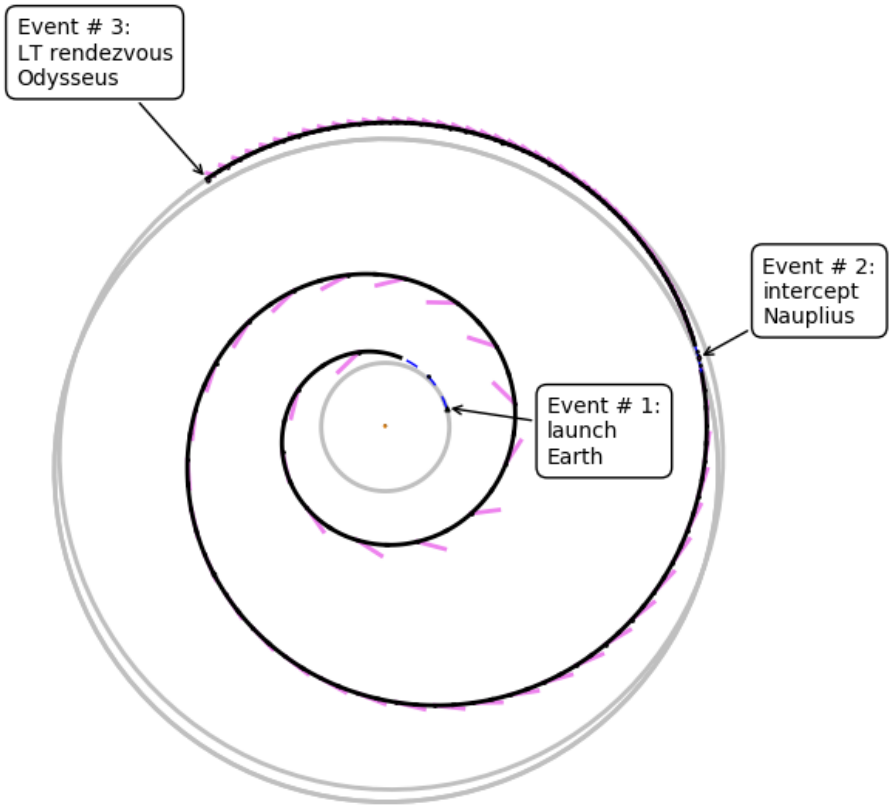

Figure 15: Optimal Trojan Tour Mission (all 4 trials qualitatively similar)

	Trial 1	Trial 2	Trial 3	Trial 4
Engine Model	2014 Discovery AO high-thrust polynomial	1-D stepped high-thrust, k = 1000	2-D stepped, k = 10000	equal area integral polynomial
Launch Date	9/15/2024	10/9/2024	9/26/2024	8/10/2024
Launch C3	12.29 km^2/s^2	9.79 km^2/s^2	10.38 km^2/s^2	8.16 km^2/s^2
Launch Mass	3107.91 kg	2935.94 kg	2954.63 kg	2999.79 kg
Nauplius Intercept Date	5/12/2033	6/15/2033	5/26/2033	5/1/2033
Nauplius Flyby v_∞	2.19 km/s	2.21 km/s	2.20 km/s	2.20 km/s
Mass at Intercept	1981.59 kg	1831.85 kg	1861.15 kg	1853.23 kg
Odysseus Arrival Date	9/15/2036	10/9/2036	9/26/2036	8/10/2036
Total Flight Time	4383 days	4383 days	4383 days	4383 days
Mass After Rendezvous	1789.21 kg	1641.01 kg	1669.70 kg	1671.17 kg
Total Propellant Use	1318.70 kg	1294.94 kg	1284.93 kg	1328.62 kg

Table 7: Trajectory data for the sample Trojan tour mission

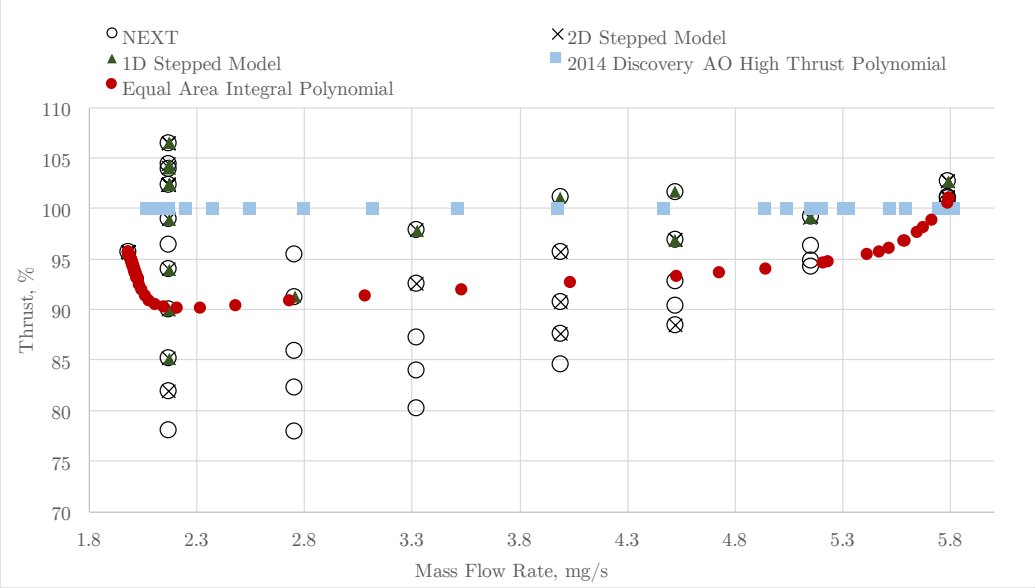

Figure 16: Comparison of Engine Model Outputs for the Sample Trojan Tour Mission. Nondimensional thrust is plotted, scaled by the value of the AO polynomial at any given mass flow rate.

CONCLUSIONS

Multiple models have been presented for improved modeling of low thrust engine performance for use with gradient based optimizers. The standard method for modeling engine performance is to create a polynomial for thrust generated and mass-flow rate of the engine as a function of input power only. This can over or under estimate performance, predict thruster outputs which are physically unrealistic, and often do not even match the throttle points that they are approximating.

For preliminary design, in order to achieve robust optimization capability, polynomials are useful nonetheless. However, better approximation of the overall performance would be acheived with a modified polynomial, such as the area integral matching method. Further, using step function approximations, optimization is possible using either a 1-D non-dominated sets of the throttle table or the full 2-dimensional table itself. The numerical challenges of generating the 2-D set however, makes it much more sensitive to the throttle sharpness, and good initial guesses are still required.

Examples were shown of realistic mission design using each of the models. Polynomial models do not accurately model performance, but improved models can get closer than the industry standard least squares regression. Further the 2-D stepped model shows improvement over the 1-D throttle sets, as the optimizer is given increased control authority.

Further testing of each stepped model is planned in order to quantify convergence and demonstrate them on a wider set of problems.

ACKNOWLEDGMENTS

The authors would like to thank Jeff Woytach of the NASA Glenn Research Center for his assistance with the most recent version of the NEXT-C throttle table.

REFERENCES

[1] "NASAs Evolutionary Xenon Thruster (NEXT): Ion Propulsion GFE Component Information Summary for Discovery Missions, July 2014," `http://discovery.larc.nasa.gov/discovery/pdf_files/20-NEXT-C_AO_Guidebook_11July14.pdf`, July 2014.

[2] "NASA's Evolutionary Xenon Thruster - Commercial (NEXT-C) Throttle Table, Baseline," September 2016.

[3] "Announcement of Opportunity: New Frontiers 4," `newfrontiers.larc.nasa.gov`, December 2016.

[4] J. A. Englander, B. A. Conway, and T. Williams, "Automated Mission Planning via Evolutionary Algorithms," *Journal of Guidance, Control, and Dynamics*, Vol. 35, nov 2012, pp. 1878–1887, 10.2514/1.54101.

[5] J. A. Englander and B. A. Conway, "An Automated Solution of the Low-Thrust Interplanetary Trajectory Problem," *Journal of Guidance, Control, and Dynamics*, 2016. Accepted.